MICROBIAL ECOLOGY

Microb Ecol (1997) 33:2–10

Spatial Distribution and Coexistence of *Klebsiella pneumoniae* and *Pseudomonas aeruginosa* in Biofilms

P.S. Stewart,[1] A.K. Camper,[2] S.D. Handran,* C.-T. Huang, M. Warnecke[3]

[1] Center for Biofilm Engineering and Department of Chemical Engineering, Montana State University–Bozeman, Bozeman, Montana 59717, USA
[2] Center for Biofilm Engineering and Department of Civil Engineering, Montana State University–Bozeman, Bozeman, Montana 59717, USA
[3] Center for Biofilm Engineering and Department of Microbiology, Montana State University–Bozeman, Bozeman, Montana 59717, USA

Received: 18 April 1996; Accepted: 23 April 1996

Abstract

The heterotrophic bacteria *Klebsiella pneumoniae* and *Pseudomonas aeruginosa* stably coexisted in laboratory-grown biofilms, even though the growth rate of *K. pneumoniae* was twice that of *P. aeruginosa* under planktonic growth conditions. The failure of *K. pneumoniae* to displace *P. aeruginosa* from the biofilm could not be attributed to concentration gradients of the limiting nutrient (glucose) arising from the interaction of reaction and diffusion. Comparisons of the growth rates of the two species in mono- and binary-population biofilms suggested partial segregation of the two species in the latter. We used a fluorescently labeled monoclonal antibody to examine the spatial distribution of *K. pneumoniae* in frozen cross sections of biofilm to confirm this segregation. *K. pneumoniae* microcolonies resided on top of, or intermixed with, a base film of *P. aeruginosa.* We hypothesize that microscale structural heterogeneity and differing rates of bacterial attachment and detachment of the two species are responsible for coexistence in this system.

Introduction

Although many microbiological investigations have focused on planktonic microorganisms, the predominant mode of microbial existence in many natural [9] and engineered environments [7] is in surface-associated biofilms. The distinction between planktonic and biofilm growth is important because the chemistry and ecologies of these two modes differ. It is known, for example, that limitation by the rate of solute diffusion can lead to concentration gradients in and around the biofilm [19]. Such mass transport considerations underpin the design of biofilm reactors used in wastewater treatment [12], may partially explain the relative resistance of biofilm microorganisms to disinfection by antimicrobial agents [22], and contribute to the ability of attached microbial colonies to induce corrosion [15].

* *Present address:* Department of Neurology, Campus Box 8111, Washington University School of Medicine, St. Louis, MO 63110.
Correspondence to: P.S. Stewart. Fax: (406) 994-6098

Table 1. Specific growth rates of *K. pneumoniae* (Kp) and *P. aeruginosa* (Pa) in planktonic culture[a]

Expt.	Kp X_0 (cfu/ml)	Pa X_0 (cfu/ml)	Kp μ (h^{-1})	Pa μ (h^{-1})
1	1.2×10^4	0	0.84 ± 0.23	—
2	0	2.7×10^4	—	0.36 ± 0.04
3	1.6×10^5	6.9×10^2	0.89 ± 0.32	0.39 ± 0.08
4	2.2×10^4	8.2×10^3	0.85 ± 0.14	0.34 ± 0.18
5	2.0×10^4	6.2×10^4	0.91 ± 0.20	0.31 ± 0.19

[a] X_0 denotes the initial cell density. The values are the means of three experiments. Specific growth rates are presented ± the standard error

Concentration gradients established through transport limitation also provide an explanation for the ecological diversity of microbial biofilms [19, 26]. Natural biofilms invariably harbor mixed populations of microorganisms. Species are thought to dominate strata within the biofilm according to their metabolic activities and the local concentrations of substrates, electron acceptors, and products. For example, anaerobes can thrive in biofilms, even when the bulk water is oxygenated, because aerobic organisms in the outer portion of the biofilm deplete dissolved oxygen [14, 19]. The mathematical theory of simultaneous reaction and diffusion predicts such concentration gradients [12, 26]. Concentration gradients in dissolved nutrients may explain some of the stratification of microbial species that has been observed in biofilms [18, 20, 25].

Concentration gradients arising from mass transport limitations are probably not the only mechanism creating microbial diversity in biofilms. In planktonic cultures, growth and death rates govern the outcome of competition. In a biofilm, the additional processes of attachment, detachment, and particulate (cell) transport will also influence species competition. In this article, we reject a reaction-diffusion explanation for the experimentally observed coexistence of bacteria in a two-species biofilm. We hypothesize, instead, that microscale structural heterogeneity and differing rates of attachment and detachment of the two species are responsible for coexistence in this system.

This research concerns a previously studied [21, 23, 24] two-species system consisting of *Pseudomonas aeruginosa* and *Klebsiella pneumoniae*. The original reasons for selecting this system included the following: (1) both species are commonly encountered in biofilms in natural and engineered environments, (2) a two-species system is simple enough to be amenable to quantitative analysis and in situ speciation, (3) both species utilize glucose as a sole carbon and energy source, (4) the two microorganisms are metabolically distinct: *P. aeruginosa* is an obligate aerobe whereas *K. pneumoniae* is facultative, and (5) *P. aeruginosa* is motile whereas *K. pneumoniae* is not. This paper reports on the spatial distribution of the two bacteria in binary population biofilms, which we have obtained by microscopic examination of specimens stained with a fluorescent immunological probe. The wider aim of this research is to integrate this new information with previous results in order to develop insight into the processes that sustain microbial diversity in biofilms.

Materials and Methods

Microorganisms and Medium

Klebsiella pneumonia KP1 and *Pseudomonas aeruginosa* ERC1 are both biofilm-forming isolates from the Center for Biofilm Engineering (Montana State University, Bozeman, Mont.) culture collection. These bacteria, which have been described in an earlier report [21], were grown aerobically using a glucose minimal medium [21]. The glucose concentration was 100 mg/liter in batch growth experiments and 25 mg/liter in biofilm experiments. The latter concentration is sufficiently low to ensure that glucose, not oxygen, was the limiting nutrient throughout the biofilm. This conclusion is based on calculation of the relative diffusive fluxes of oxygen and glucose [28]. The calculation has been confirmed by microelectrode measurements of dissolved oxygen profiles within the biofilm, which show that oxygen permeates the biofilm at concentrations everywhere greater than 4 mg/liter [23].

Planktonic Culture

Batch cultures were grown in 100 ml of medium in 250-ml flasks shaken at 200 rpm. Overnight cultures of *P. aeruginosa* and *K. pneumoniae* were enumerated by acridine orange direct counts before inoculation. Different proportions of *P. aeruginosa* and *K. pneumoniae* were inoculated into 50 ml of medium in five separate experiments (Table 1). The culture was sampled periodically for viable cell counts. *P. aeruginosa* was enumerated on *Pseudomonas* isolation agar (Difco, Detroit, MI) plates incubated at 35°C for 24 h. *K. pneumoniae* was enumerated on R2A agar (Difco, Detroit, MI) plates incubated at 35°C for 8 h, after which only *K. pneumoniae* colonies were detectable.

Biofilm Culture

Biofilm was grown in continuous flow annular reactors [21]. The reactors had a working volume of approximately 600 ml, a wetted surface area of 0.19 m^2, and were operated at dilution rates of 3.2 h^{-1}. Reactors were inoculated for 12 h using the combined flow of individual chemostats growing either *P. aeruginosa* or *K. pneumoniae*. Twelve removable stainless steel slides (1.7 × 19 cm) allowed sampling of biofilm from the annular reactor. After 5 days of

operation, three slides were removed and one each used for viable cell counts, direct confocal microscopic observation, and fluorescent antibody staining.

Monoclonal Antibody Preparation and Evaluation

K. pneumoniae whole cell preparations were fixed in 0.5% paraformaldehyde for 5 min, pelleted by centrifugation, and resuspended in phosphate-buffered saline. They were then emulsified in complete Freund's adjuvant for primary immunization and in incomplete Freund's adjuvant for the second and third immunizations. Female Sprague-Dawley rats were inoculated intraperitoneally with 100–500 μl of the antigen preparation, and given two additional immunizations at 2-week intervals. Four days prior to fusion, the rats were boosted with fixed whole bacteria without adjuvant. Rats were sacrificed; the spleen was removed, homogenized, and fused with Sp 2/0 mouse myeloma cells. Nine hundred sixty hybridoma supernatants were screened by ELISA and immunofluorescence assay (IFA) for the selective staining of the target bacterial cells. Two monoclonal antibody supernatants, with bright staining, were selected for further analysis by flow cytometry.

Bacteria used for flow cytometry analysis of the hybridoma supernatants were fixed in 0.5% paraformaldehyde for 5 min, centrifuged, and resuspended in phosphate-buffered saline (PBS). The cells were incubated with hybridoma supernatant for 30 min on ice, washed three times in PBS containing 2% rabbit serum, incubated with goat anti-rat IgG FITC conjugate for 30 min on ice, washed as before, and analyzed with a flow cytometer (FACScan, Becton-Dickinson, Cockeysville, MD). Autofluorescence of cell preparations was measured by sampling untreated cells, and nonspecific binding of the secondary antibody was measured by reacting cells to the goat anti-rat IgG FITC–conjugated antibody. The monoclonal antibody giving the highest signal was used in these experiments.

Additional tests were done to assess the specificity of the monoclonal, and the effects of target cell growth conditions, on antigen expression. In the latter case, *K. pneumoniae* was grown in either low (72 μM glucose) or high (tryptic soy broth [TSB], Difco) carbon concentration batch cultures. These cells were harvested by centrifugation, washed, stained, and the staining intensity determined by flow cytometry. Starved cells were also prepared by initially growing the bacteria in one-tenth-concentration TSB, followed by washing and resuspension in PBS. The culture was held at room temperature for 5 days prior to staining as above. The influence of biofilm growth on antigen expression was assessed by scraping pure culture biofilms of *K. pneumoniae* from annular reactor slides, followed by dispersion, staining, and flow cytometry. Regardless of the growth conditions, the antibody reacted with the cells and produced a high fluorescent signal (300 arbitrary fluorescence units). The antibody did not react with seven other *K. pneumoniae* isolates, nor did it cross-react with the *P. aeruginosa,* as determined by flow cytometry (less than 10 arbitrary fluorescence units), ELISA, or IFA.

Antibody Staining and Microscopy

The spatial distribution of bacterial species in biofilm was investigated using an immunofluorescence technique. To examine species distribution within the biofilm, 5-μm-thick cross sections of frozen biofilm were prepared, as described elsewhere [29]. These sections were affixed to polylysine-coated glass slides, then fixed in 1% paraformaldehyde. Samples were immersed in a blocking solution consisting of 2% skim milk and 0.3% Tween 80 in Tris-buffered saline (TBS). The slide was then transferred to a primary antibody solution (anti-*Klebsiella* monoclonal raised in rat), followed by a secondary antibody solution (FITC-labeled anti-rat raised in goat, Fisher Scientific, Pittsburgh, PA), followed by a 50-μg/ml propidium iodide (Sigma, St. Louis, MO) solution. Each step was separated by three washes of 0.03% Tween 80 in pH 7.4 TBS; this same solution was also used to dilute the antibodies and propidium iodide. The pH was adjusted to 9 prior to microscopic examination. Stained sections were viewed with an Olympus BH-2 microscope (Olympus, Lake Success, NY) with an optical train consisting of an excitation filter (BP490), a dichroic mirror (DM500), and a barrier filter (AFC+0515). FITC-labeled *K. pneumoniae* exhibited a green or yellow fluorescence, and propidium iodide–stained bacteria were red (*P. aeruginosa*). To examine the lateral distribution of microorganisms, intact biofilm was fixed in 1% paraformaldehyde and treated with a blocking agent, as above. The intact biofilm was then stained, as described for the cross sections. The hydrated biofilm was examined by confocal scanning laser microscopy (BioRad MRC 600 dual krypton/argon laser) using a 100× 1.2 n.a. water immersible objective. Simultaneous images from both laser channels were collected at 5-μm intervals from the surface of the biofilm. At each interval, individual digital images were captured and stored electronically.

These methods were used for monopopulation control biofilms, as well as the experimental binary population biofilms. In the case of a single-species *K. pneumoniae* biofilm, uniform antibody staining was observed. AS predicted with the flow cytometry cross-reactivity studies, there was no antibody staining of the pure culture *P. aeruginosa* biofilms. In both cases, propidium iodide staining was uniformally bright throughout the sample.

Mathematical Modeling

A computer model of biofilm population dynamics was used to simulate competition of two species in a biofilm. The model implements the conceptual and mathematical formulation described by Wanner and Gujer [26]. Incorporated into the model are processes of bulk flow in and out of the reactor, diffusion of glucose within the biofilm, glucose consumption by bacterial metabolism, bacterial growth, advection of cell mass within the biofilm, and cell detachment. Key assumptions embodied in this model include the following: (1) the biofilm is uniformly thick, (2) the overall volume fraction occupied by cells in the biofilm is constant, and (3) biofilm species composition is homogenous in the direction parallel to the substratum. Parameter values used in the simulation and their respective references are tabulated in Table 2.

Results

Klebsiella pneumoniae consistently grew at twice the rate of *Pseudomonas aeruginosa* in glucose-limited planktonic cul-

Table 2. Parameter values and sources for biofilm population dynamics modeling[a]

Parameter	Value	Source[b]
Maximum specific growth rate, Kp	48 d^{-1}	a
Maximum specific growth rate, Pa	6.7 d^{-1}	6
Monod coefficient, Kp	3.5 g m^{-3}	a
Monod coefficient, Pa	5.0 g m^{-3}	6
Yield coefficient, Kp	0.032 g g^{-1}	a
Yield coefficient, Pa	0.096 g g^{-1}	1
Cell volume fraction	0.05	8[c]
Cell intrinsic density	400,000 g m^{-3}	3
Initial biofilm thickness	25 μm	21
Concentration boundary layer thickness	1 μm	11
Initial volume fraction, Kp	0.01	21
Initial volume fraction, Pa	0.04	21
Substrate influent concentration	25 g m^{-3}	21
Glucose diffusion coefficient	5.43×10^{-5} m^2 d^{-1}	17
Biofilm/bulk diffusivity ratio	0.8	27
Surface area to volume ratio	365 m^{-1}	a
Dilution rate	145 d^{-1}	a

[a] Species-specific values are denoted by Kp (*K. pneumoniae*) and Pa (*P. aeruginosa*)

[b] Numbers indicate the reference number; a, Siebel, MA (1987) Binary population biofilms, PhD thesis, Montana State University, Bozeman, Mon

[c] Calculated assuming a typical biofilm cell density of 20,000 g m^{-3}

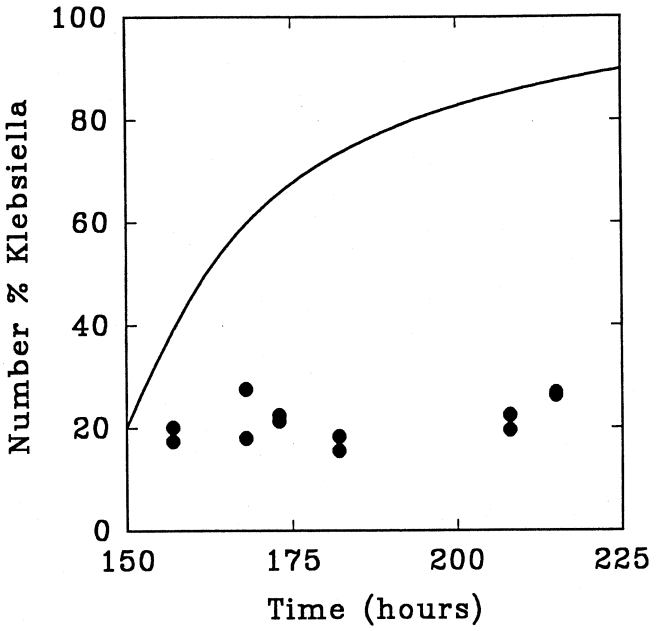

Fig. 1. Competition of *K. pneumoniae* and *P. aeruginosa* in a biofilm. Data of Seibel and Characklis (●, ref. [21]) are compared to a computer model simulation (—). The simulation was initiated at time equal to 150 h.

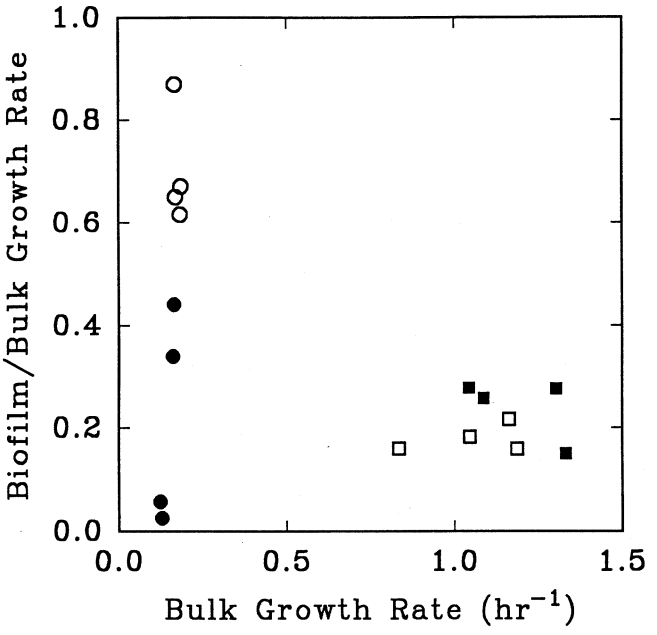

Fig. 2. Comparison of microbial growth rates in monopopulation and binary population biofilms. Data of Siebel [21] were analyzed to compare the average specific growth rate in biofilms, determined by an overall material balance on cell mass, with the growth rate expected based on the bulk concentration of glucose and known kinetic parameters. *K. pneumoniae* exhibits about the same reduction in either monopopulation (□) or binary population biofilms (■). *P. aeruginosa* fares worse in the binary population film (●) than in the monopopulation biofilm (○). The points are individual values each from a separate annular reactor experiment.

ture experiments (Table 1). The average specific growth rate in four experiments was 0.87 h^{-1} and 0.35 h^{-1} for *K. pneumoniae* and *P. aeruginosa,* respectively. There was no evidence of any species interactions from the planktonic culture experiments; both microorganisms grew at the same rate in the presence of the other species as they did in pure culture. The relative growth rates of the two microorganisms measured in this study are qualitatively consistent with previously determined kinetic parameters (maximum specific growth rate and Monod coefficient) for these two microorganisms (Table 2). From these parameters, *K. pneumoniae* was predicted to grow from five to seven times faster than *P. aeruginosa,* regardless of the glucose concentration. It was also found, in previous work, that Monod kinetic parameters were not altered by growth in biofilms [1, 21].

According to conceptual and mathematical descriptions of biofilm population dynamics that treat the biofilm as a uniformly thick and laterally homogenous slab [26], *K. pneumoniae* should outcompete *P. aeruginosa* in glucose-limited biofilm cultures due to its higher growth rate. To test

this hypothesis, we performed a computer simulation of biofilm species competition for these two microorganisms (Fig. 1). Since *K. pneumoniae* has a higher growth rate, the model predicts displacement of *P. aeruginosa* from all regions of the biofilm. This simulation did predict rapid dominance by *K. pneumoniae* that is inconsistent with the stable coexistence observed by Siebel and Characklis [21] and reproduced in this work (Fig. 1). Thus, a reaction-diffusion explanation for biofilm coexistence is not tenable in this system.

One possible explanation for the insufficiency of this mathematical model is that it assumes a simple, uniformly thick biofilm and a laterally homogeneous distribution of microbial species. Natural biofilms, when examined microscopically, reveal rough surfaces and local segregation of microbial species [10, 16]. Such microscale structural heterogeneity should allow microbial species to attach and detach from the biofilm at independent rates, thereby altering the mathematical rules governing biofilm population dynamics [2, 4, 11, 13]. In the uniformly thick biofilm model, all species detach at the same rate, permitting the fastest growing species in a given stratum to out compete other microorganisms. In a structurally heterogeneous biofilm, there is no reason to expect the rates of species attachment and detachment to be the same. In such a system, a microorganism could persist by virtue of slow detachment as successfully as by rapid growth. In other words, the assumption of uniform biofilm thickness, while adequate in many modeling applications, may be inadequate to completely account for biofilm population dynamics.

The specific growth rates of the two species in monopopulation and binary population biofilms, developed under identical substrate loading conditions, were compared to gain an understanding of the structure of binary population biofilms. The ratio of the average specific growth rate in the biofilm to the specific growth rate at bulk solution condi-

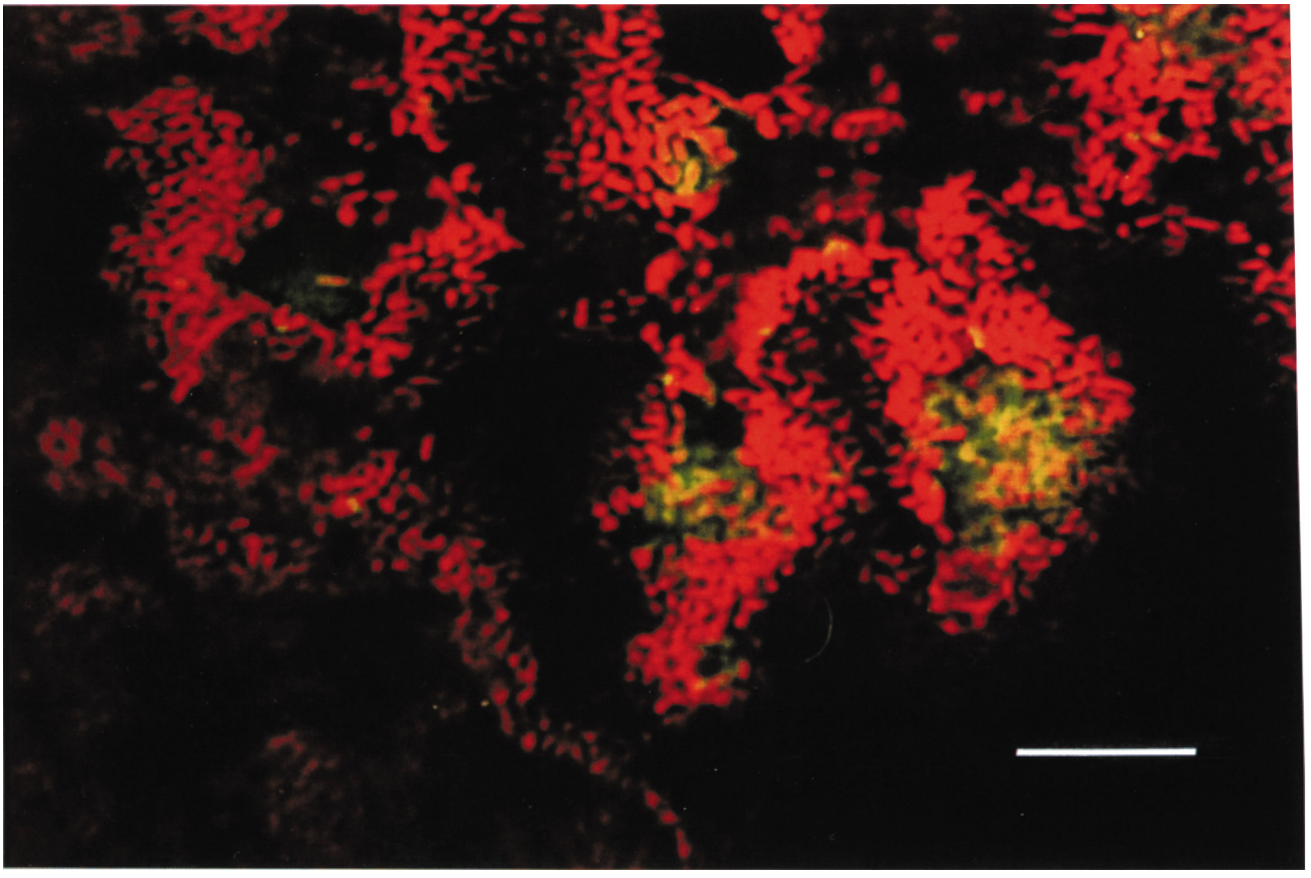

Fig. 3. Confocal scanning laser micrograph showing distribution of *K. pneumoniae* in biofilm, plan view (pseudo-color). Green indicates fluorescein fluorescence and the presence of *K. pneumoniae;* red indicates propidium iodide, which stains nucleic acids of either bacterial species. Regions lacking green fluorescence indicate the presence of *P. aeruginosa* alone.

tions reflects the extent to which mass transport limits the growth rate of biofilm bacteria. Experimental measurements of this ratio, as calculated from the original data of Siebel and Characklis [21], range from about 0.05 to 0.85 (Fig. 2). The mean ratio for *P. aeruginosa* in their monopopulation biofilms was 0.70, indicating little mass transport limitation. The mean ratio for *P. aeruginosa* in binary population biofilms, however, was 0.22. The means are significantly different ($P = 0.006$) showing that *P. aeruginosa* grows more slowly in the binary population biofilm that it does in a pure culture biofilm. In contrast, the mean ratios of biofilm and bulk growth rates for *K. pneumoniae* in the two types of biofilms are not different at the 95% confidence level ($P = 0.117$). (Fig. 2).

The reanalysis of Siebel and Characklis's data, shown in Fig. 2, suggests a structural model of the biofilm in which microcolonies of *K. pneumoniae* are dispersed on the surface of a base film of *P. aeruginosa.* The *K. pneumoniae* microcolonies would partially obscure underlying *P. aeruginosa,* causing the observed discrepancy in growth rates between the binary and monopopulation biofilm experiments. Conversely, the *K. pneumoniae* microcolonies remain near the biofilm–bulk water interface where they are not hindered by mass transport limitation, and therefore grow at the same rate in mono- and binary-population biofilms. Implicit in such a structural model is the ability of the *K. pneumoniae* to attach to the *P. aeruginosa* film from the bulk solution. Development of this biofilm structure could also be due, in part, to the motility of the two organisms. It has been shown that motile *P. aeruginosa* attaches to a clean surface in a random pattern [5]. Maximum surface coverage of 10% was attained within 6 h for the *P. aeruginosa,* while colonization of a clean surface by the nonmotile *K. pneumoniae* was extremely sporadic, even after 24 h (unpublished data). Once growth of the attached organisms began, the *K. pneumoniae* could persist in the biofilm by virtue of its faster growth rate and its ability to attach to the *P. aeruginosa* film. This hypothesis is, in part, substantiated by observations made by Siebel and Characklis where putative "towers" of *K. pneumoniae* protruded above the base biofilm [21]. A limitation of their research was the inability to differentiate the two bacterial species in an intact biofilm.

We were able to directly observe heterogeneity in the spatial distributions of the two species by probing intact and cryosectioned binary population biofilms with a FITC-conjugated monoclonal antibody against *K. pneumoniae.* Plan view images of stained biofilms revealed an uneven biofilm in which localized microcolonies of *Klebsiella* appeared on a background of *Pseudomonas* (Fig. 3). To quantify the variable distribution of *K. pneumoniae,* the average intensity of propidium iodide and fluorescein staining were compared at 10 randomly selected areas of the specimen (Table 3). The coefficient of variation of the averaged intensity of propidium iodide (which stains nucleic acids of both species) in a selected area was 0.26. The ratio of fluorescein to propidium iodide intensity in the same 10 regions had a coefficient of variation of 0.8, representing the relative proportion of *K. pneumoniae.* This indicates much greater local variability in the species composition of the biofilm than in the total amount of biomass.

The spatial heterogeneity observed in the plan images was substantiated in antibody-stained, cryosectioned binary population biofilms (Fig. 4). Long stretches of biofilm stained only with propidium iodide (Fig. 4A), indicating the presence of *P. aeruginosa* alone. The pure *P. aeruginosa* portions of the biofilm were approximately the same thickness (20–30 μm). This is consistent with previous measurements of these biofilms grown under similar conditions [16]. In regions where fluorescein fluorescence indicated the presence of *K. pneumoniae* (Fig. 4B,C), the biofilm was locally thicker by as much as a factor of 2. In some instances, the *K. pneumoniae* appeared to be a distinct colony above a *P. aeruginosa* base film (Fig. 4C). In other areas, *K. pneumoniae* and *P. aeruginosa* were partially intermixed from the surface to the substratum (Fig. 4B).

Discussion

Based on our observations, we propose the following conceptual model for coexistence of the two species of bacteria

Table 3. Area-averaged propidium iodide (PI) and FITC-conjugated (F) anti–*K. pneumoniae* staining of binary population biofilm[a]

Area no.	PI	F/PI
1	0.39	0.004
2	0.42	0.043
3	0.57	0.015
4	0.23	0.180
5	0.69	0.006
6	0.49	0.089
7	0.59	0.051
8	0.58	0.166
9	0.50	0.176
10	0.37	0.116
Mean	0.48	0.085
CoV	0.26	0.80

[a] The averaging area was a rectangular area in the plane of the substratum of approximately 1×10^4 μm^2. The units of intensity are arbitrary. The coefficient of variation (CoV) is the standard deviation divided by the mean

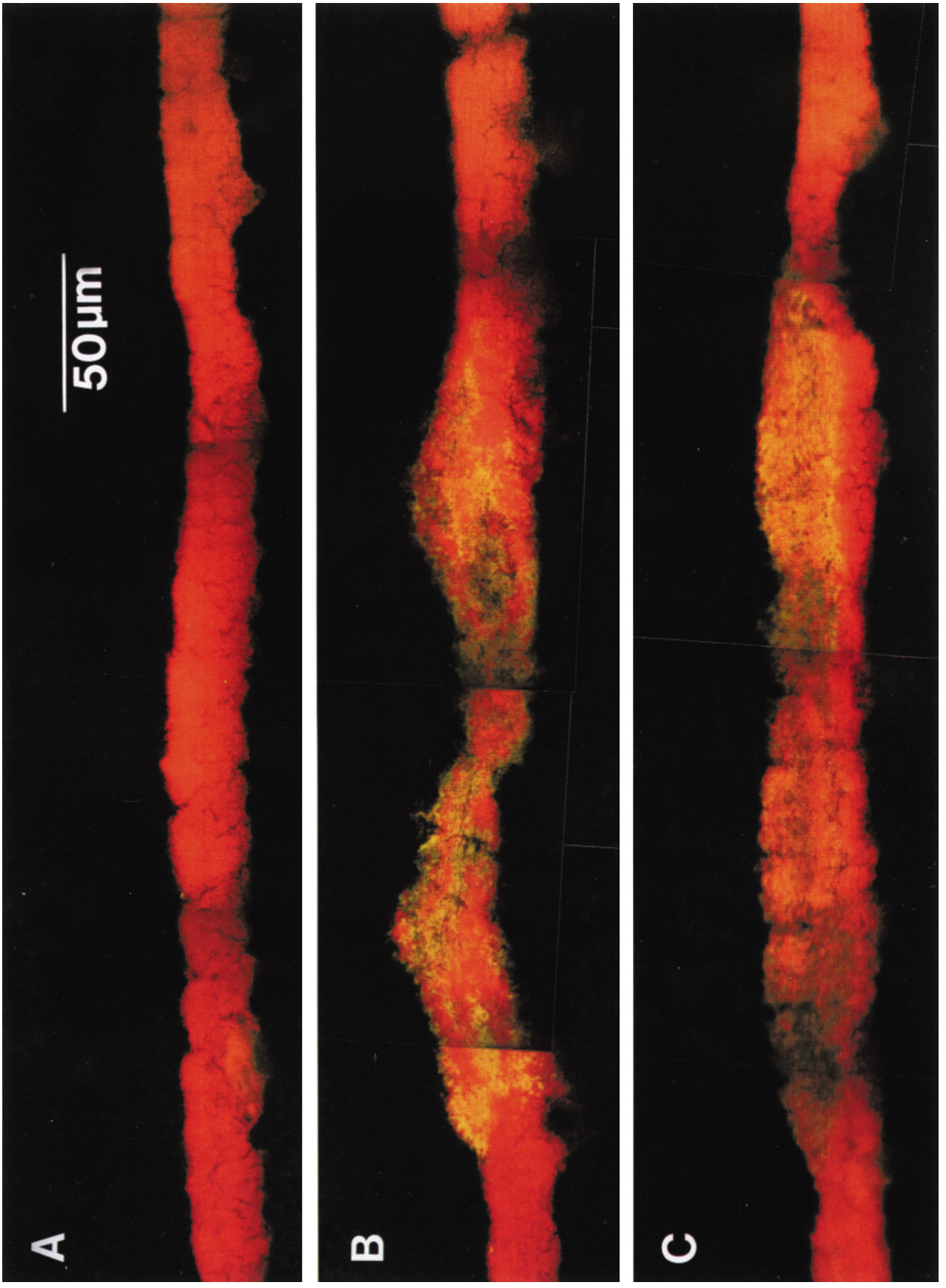

Fig. 4. Photomicrographic montage showing distribution of *K. pneumoniae* in biofilm cross sections. Green indicates fluorescein fluorescence and the presence of *K. pneumoniae;* red indicates propidium iodide, which stains nucleic acids of either bacterial species. Regions lacking green fluorescence indicate the presence of *P. aeruginosa* alone. Where fluorescence from propidium iodide and fluorescein overlap the color appears yellow; this indicates the presence of *K. pneumoniae* alone or a mixture of *K. pneumoniae* and *P. aeruginosa.*

in this biofilm system. Although an equal number of both species were inoculated simultaneously, *P. aeruginosa* colonizes the substratum more rapidly. Studies of initial attachment by these two microorganisms support this assertion (unpublished data). *P. aeruginosa* thus becomes a permanent member of the biofilm. In contrast, *K. pneumoniae* attaches to the *P. aeruginosa* base film and persists by virtue of a higher growth rate. This conceptual model supports the previous data that suggest the two organisms coexist and is consistent with the observed microscale spatial distribution of the two species.

In summary, *K. pneumoniae* and *P. aeruginosa* coexist in glucose-limited biofilms even though *K. pneumoniae* has a higher growth rate than *P. aeruginosa.* The data presented suggest that this coexistence cannot be attributed exclusively to mass transport phenomena. Rather, initial attachment events and biofilm microscale structural heterogeneity are likely to be important in determining biofilm ecology. In addition, our results suggest that slower growing *P. aeruginosa* persists because of its ability to rapidly colonize the substratum and thereby establish a long-term competitive advantage. *K. pneumoniae* thrives by virtue of its ability to attach to the base film and outcompete the *P. aeruginosa* in the surface layers of the biofilm. Structural heterogeneity allows attachment of microorganisms in the biofilm interior and uncouples the detachment rates of competing microorganisms, thus fundamentally altering biofilm population dynamics.

The relevance of these hypotheses to other biofilm ecosystems are unclear, since they were drawn from observations of a laboratory model system. A full understanding of biofilm population dynamics in any system will require more sophisticated descriptions of biofilm topography and the processes of particulate attachment and detachment.

Acknowledgments

This work was supported through cooperative agreement EEC-8907039 between the National Science Foundation and Montana State University and by the industrial partners of the Center for Biofilm Engineering. We thank Kathy Jutila and Dr. Mark Jutila from the Department of Veterinary and Molecular Biology at Montana State University for their assistance in the preparation and testing of the monoclonal antibody, Dr. Cliff Bond and Garth James for help in optimizing the antibody staining of biofilms, and Paul Stoodley for assistance with the confocal scanning laser microscope.

References

1. Bakke R, Trulear MG, Robinson JA, Characklis WG (1984) Activity of *Pseudomonas aeruginosa* in biofilms: steady state. Biotechnol Bioeng 26:1418–550
2. Baltzis BC, Fredrickson AG (1983) Competition of two microbial populations for a single resource in a chemostat when one of them exhibits wall attachment. Biotechnol Bioeng 25: 2419–2439
3. Bratbak G, Dundas I (1984) Bacterial dry matter content and biomass estimations. Appl Environ Microbiol 48:755–757
4. Bryers JD (1984) Biofilm formation and chemostat dynamics: pure and mixed culture considerations. Biotechnol Bioeng 26: 948–958
5. Camper AK, Hamilton MA, Johnson KR, Stoodley P, Harkin GJ, Daly DS (1994) Bacterial colonization of surfaces in flowing systems: methods and analysis. Ultrapure Water 11:27–36
6. Characklis WG (1990) Kinetics of microbial transformations. In: Characklis WG, Marshall KC (eds) Biofilms. Wiley, New York, pp 233–264
7. Characklis WG, Marshall KC (1990) Biofilms: a basis for an interdisciplinary approach. In: Characklis WG, Marshall KC (eds) Biofilms. Wiley, New York, pp 3–15
8. Christensen BE, Characklis WG (1990) Physical and chemical properties of biofilms. In: Characklis WG, Marshall KC (eds) Biofilms. Wiley, New York, pp 93–130
9. Costerton JW, Cheng KJ, Geesey GG, Ladd TI, Nickel JC, Dasgupta M, Marrie TJ (1987) Bacterial biofilms in nature and disease. Annu Rev Microbiol 41:435–464
10. Costerton JW, Lewandowski Z, deBeer D, Caldwell D, Korber D, James G (1994) Biofilms, the customized microniche. J Bacteriol 176:2137–2142
11. Drury WJ, Stewart PS, Characklis WG (1993) Transport of 1-μm latex particles in *Pseudomonas aeruginosa* biofilms. Biotechnol Bioeng 42:111–117
12. Grady CPL Jr, Lim HC (1980) Biological wastewater treatment theory and applications. Marcel Dekker, New York
13. Gujer W (1987) The significance of segregation of biomass in biofilms. Water Sci Technol 19:495–503
14. Kühl M, Jørgensen BB (1992) Microsensor measurements of sulfate reduction and sulfide oxidation in compact microbial communities of aerobic biofilms. Appl Environ Microbiol 58: 1164–1174
15. Little BJ, Wagner PA, Characklis WG, Lee W (1990) Microbial corrosion. In: Characklis WG, Marshall KC (eds) Biofilms. Wiley, New York, pp 635–670
16. Murga R, Stewart PS, Daly D (1995) Quantitative analysis of biofilm thickness variability. Biotechnol Bioeng 45:503–510
17. Perry RH, Chilton CH (1973) Chemical engineer's handbook, 5th edn. McGraw-Hill, New York, pp 3–222
18. Ramsing NB, Kühl M, Jørgensen BB (1993) Distribution of sulfate-reducing bacteria, O_2, and H_2S in photosynthetic biofilms determined by oligonucleotide probes and microelectrodes. Appl Environ Microbiol 59:3840–3849

19. Revsbech NP, Jørgensen BB (1986) Microelectrodes: their use in microbial ecology. Adv Microb Ecol 9:293–352
20. Robinson RW, Akin DE, Nordstedt RA, Thomas MV, Aldrich HC (1984) Light and electron microscopic examinations of methane-producing biofilms from anaerobic fixed-bed reactors. Appl Environ Microbiol 48:127–136
21. Siebel MA, Characklis WG (1991) Observations of binary population biofilms. Biotechnol Bioeng 37:778–789
22. Stewart PS, Raquepas JB (1995) Implications of reaction-diffusion theory for the disinfection of microbial biofilms by reactive antimicrobial agents. Chem Eng Sci 50:3099–3104
23. Stewart PS, Griebe T, Srinivasan R, Chen C-I, Yu FP, deBeer D, McFeters GA (1994) Comparison of respiratory activity and culturability during monochloramine disinfection of binary population biofilms. Appl Environ Microbiol 60:1690–1692
24. Sturman PJ, Jones WL, Characklis WG (1994) Interspecies competition in colonized porous pellets. Water Res 28:831–839
25. Tanaka H, Dunn IJ (1982) Kinetics of biofilm nitrification. Biotechnol Bioeng 24:669–689
26. Wanner O, Gujer W (1986) A multispecies biofilm model. Biotechnol Bioeng 28:314–328
27. Westrin BA, Axelson A (1991) Diffusion in gels containing immobilized cells: a critical review. Biotechnol Bioeng 38:439–446
28. Williamson K, McCarty P (1976) A model of substrate utilization by bacterial films. J Water Pathol Cont Fed 48:9–24
29. Yu FP, Callis GM, Stewart PS, Griebe T, McFeters GA (1994) Cryosectioning of biofilm for microscopic examination. Biofouling 8:85–91